

Variation of hadron masses in finite nuclei

K. Saito*

Physics Division, Tohoku College of Pharmacy

Sendai 981, Japan

K. Tsushima[†] and A. W. Thomas[‡]

Department of Physics and Mathematical Physics

University of Adelaide, South Australia, 5005, Australia

Abstract

The quark-meson coupling model, based on a mean-field description of non-overlapping nucleon bags bound by the self-consistent exchange of σ , ω and ρ mesons, is extended to investigate the change of hadron properties in finite nuclei. Relativistic Hartree equations for spherical nuclei have been derived from a relativistic quark model of the structure of bound nucleons and mesons. Using this unified, self-consistent description of both infinite nuclear matter and finite nuclei, we investigate the properties of some closed-shell nuclei, and study the changes in the hadron masses of the non-strange vector mesons, the hyperons and the nucleon in those nuclei. We find a new, simple scaling relation for the changes of the hadron masses, which can be described in terms of the number of non-strange quarks in the hadron and the value of the scalar mean-field in a nucleus.

PACS numbers: 12.39.Ba, 21.60.-n, 21.90.+f, 24.85.+p

*ksaito@nucl.phys.tohoku.ac.jp

†ktsushim@physics.adelaide.edu.au

‡athomas@physics.adelaide.edu.au

I INTRODUCTION

One of the most exciting topics in nuclear physics is the study of the variation of hadron properties as the nuclear environment changes. In particular, the medium modification of the light vector-mesons is receiving a lot of attention, both theoretically and experimentally. Recent experiments from the HELIOS-3 [1] and the CERES [2] collaborations at the SPS/CERN energies have shown that there exists a large excess of the e^+e^- pairs in central S + Au collisions. Those experimental results may give a hint of some change of hadron properties in nuclei [3]. Forthcoming, ultra-relativistic heavy-ion experiments (eg. at RHIC) are also expected to give significant information on the strong interaction (QCD), through the detection of changes in hadronic properties (for a review, see Ref.[4]).

Theoretically, lattice QCD simulations may eventually give the most reliable information on the density and/or temperature dependence of hadron properties in matter. However, current simulations have been performed only for finite temperature systems with zero baryon density [5]. Therefore, many authors have studied the hadron masses in matter using effective theories: the vector dominance model [6], QCD sum rules [7] and the Walecka model [8, 9, 10, 11], and have reported that the mass decreases in the nuclear medium (see also Ref.[12]).

In the approach based on QCD sum rules, the reduction of the mass is mainly due to the four-quark condensates and one of the twist-2 condensates. However, it has been suggested that there may be considerable, intrinsic uncertainty in the standard assumptions underlying the QCD sum-rule analyses [13]. In hadronic models, like Quantum hadrodynamics (QHD) [14], the on-shell properties of the scalar (σ) and vector (ω) meson with vacuum polarization were first studied by Saito, Maruyama and Soutome [8], and later by many authors [9, 10, 11]. (Good physical arguments concerning the ω meson in medium were found in Ref.[10].) The main reason for the reduction in masses in QHD is the polarization of the Dirac sea, where the *anti-nucleons* in matter play a crucial role. From the point of view of the quark model, however, the strong excitation of $N-\bar{N}$ pairs in medium is difficult to understand [15].

Recently Guichon, Saito, Rodionov and Thomas [16] have developed an entirely different model for both nuclear matter and finite nuclei, in which quarks in non-overlapping nucleon bags interact *self-consistently* with (structureless) scalar (σ) and vector (ω and ρ) mesons in the mean-field approximation (MFA) – the quark-meson coupling (QMC) model. (The original idea was proposed by Guichon in 1988 [17]. Several interesting applications to the properties of nuclear matter and finite nuclei are also given in a series of papers by Saito and Thomas [15, 18, 19, 20].) This model was recently used to calculate detailed properties of static, closed shell nuclei from ^{16}O to ^{208}Pb , where it was shown that the model can reproduce fairly well the observed charge density distributions, neutron density distributions etc. [21]. Blunden and Miller [22] have also considered a model for finite nuclei along this line.

To investigate the properties of hadrons, particularly the changes in their masses in nuclear medium, one must also consider the structure of the mesons, as well as the nucleon. Saito and Thomas [20] have studied variations of hadron masses and matter properties in *infinite* nuclear matter, in which the vector-mesons are also described by bags, but the scalar-meson mass is kept constant, and have shown the decrease of the hadron mass. Now it would be most desirable to extend this picture to *finite* nuclei to study the changes of hadron properties in the medium, *quantitatively*.

Our main aim in this paper is to give an effective Lagrangian density for finite nuclei, in which the structure effects of the mesons (σ , ω and ρ) as well as the nucleon are involved, and to study quantitative changes in the hadron (including the hyperon) masses by solving relativistic Hartree equations for spherical nuclei derived from the Lagrangian density. (Using this model, we also calculate some static properties of closed-shell nuclei.) In the present model the change in the hadron mass can be described by a simple formula, which is expressed in terms of the number of non-strange quarks and the value of the scalar mean-field (see also Ref.[20]). This is accurate over a wide range of nuclear density. We then find a new, simple scaling relation for the changes of hadron masses in the medium:

$$\frac{\delta m_{\omega,\rho}^*}{\delta M_N^*} \sim \frac{\delta M_{\Lambda,\Sigma}^*}{\delta M_N^*} \sim \frac{2}{3}, \quad \frac{\delta M_{\Xi}^*}{\delta M_N^*} \sim \frac{1}{3}, \quad \text{etc.} \quad (1)$$

where $\delta M_i^* \equiv M_i - M_i^*$, with the effective hadron mass, M_i^* ($i = N, \omega, \rho, \dots$).

An outline of the paper is as follows. In Sec. II, the idea of the QMC model is first reviewed. Then, the model is extended to include the effect of meson structure. In Sec. III, parameters in the model are first determined to reproduce the properties of infinite nuclear matter, and the hadron masses in the medium are then discussed. A new scaling relationship among them is also derived. The static properties of several closed-shell nuclei are studied in subsection III.3, where we also show the changes of the masses of the nucleon, the mesons (σ , ω and ρ) and the hyperons (Λ , Σ and Ξ) in ^{40}Ca and ^{208}Pb . The last section gives our conclusions.

II THE QUARK-MESON COUPLING MODEL

II.1 Effect of nucleon structure in finite nuclei

Let us suppose that a free nucleon (at the origin) consists of three light (u and d) quarks under a (Lorentz scalar) confinement potential, V_c . Then, the Dirac equation for the quark field, ψ_q , is given by

$$[i\gamma \cdot \partial - m_q - V_c(r)]\psi_q(r) = 0, \quad (2)$$

where m_q is the bare quark mass.

Next we consider how Eq.(2) is modified when the nucleon is bound in static, uniformly distributed (iso-symmetric) nuclear matter. In the QMC model [17] it is assumed that each quark feels scalar, V_s^q , and vector, V_v^q , potentials, which are generated by the surrounding nucleons, as well as the confinement potential (see also Ref.[22]). Since the typical distance between two nucleons around normal nuclear density ($\rho_0 = 0.15 \text{ fm}^{-3}$) is surely larger than the typical size of the nucleon (the radius R_N is about 0.8 fm), the interaction (except for the short-range part) between the nucleons should be colour singlet; e.g., a meson-exchange potential. Therefore, this assumption seems appropriate when the baryon density, ρ_B , is not high. If we use the mean-field approximation for the meson

fields, Eq.(2) may be rewritten as

$$[i\gamma \cdot \partial - (m_q - V_s^q) - V_c(\vec{r}) - \gamma_0 V_v^q]\psi_q(\vec{r}) = 0. \quad (3)$$

The potentials generated by the medium are constants because the matter distributes uniformly. As the nucleon is static, the time-derivative operator in the Dirac equation can be replaced by the quark energy, $-i\epsilon_q$. By analogy with the procedure applied to the nucleon in QHD [14], if we introduce the effective quark mass by $m_q^* = m_q - V_s^q$, the Dirac equation, Eq.(3), can be rewritten in the same form as that in free space, with the mass m_q^* and the energy $\epsilon_q - V_v^q$, instead of m_q and ϵ_q . In other words, the vector interaction has *no effect on the nucleon structure* except for an overall phase in the quark wave function, which gives a shift in the nucleon energy. This fact *does not* depend on how to choose the confinement potential, V_c . Then, the nucleon energy (at rest), E_N , in the medium is [19]

$$E_N = M_N^*(V_s^q) + 3V_v^q, \quad (4)$$

where the effective nucleon mass, M_N^* , depends on *only the scalar potential* in the medium.

Now we extend this idea to finite nuclei. The solution of the general problem of a composite, quantum particle moving in background scalar and vector fields that vary with position is extremely difficult. One has, however, a chance to solve the particular problem of interest to us, namely light quarks confined in a nucleon which is itself bound in a finite nucleus, only because the nucleon motion is relatively slow and the quarks highly relativistic [16]. Thus the Born-Oppenheimer approximation, in which the nucleon internal structure has time to adjust to the local fields, is naturally suited to the problem. It is relatively easy to establish that the method should be reliable at the level of a few percent [16].

Even within the Born-Oppenheimer approximation, the nuclear surface gives rise to external fields that may vary appreciably across the finite size of the nucleon. Our approach in Ref.[16] was to start with a classical nucleon and to allow its internal structure to adjust to minimise the energy of three quarks in the ground-state of a system under

constant scalar and vector fields, with values equal to those at the centre of the nucleon. In Ref.[16], the MIT bag model was used to describe the nucleon structure. Blunden and Miller have also examined a relativistic oscillator model as an alternative model [22]. Of course, the major problem with the MIT bag (as with many other relativistic models of nucleon structure) is that it is difficult to boost. We therefore solve the bag equations in the instantaneous rest frame (IRF) of the nucleon – using a standard Lorentz transformation to find the energy and momentum of the classical nucleon bag in the nuclear rest frame. Having solved the problem using the meson fields at the centre of the “nucleon” (which is a quasi-particle with nucleon quantum numbers), one can use perturbation theory to correct for the variation of the scalar and vector fields across the nucleon bag. In first order perturbation theory only the spatial components of the vector potential give a non-vanishing contribution. (Note that, although in the nuclear rest frame only the time component of the vector field is non-zero, in the IRF of the nucleon there are also non-vanishing spatial components.) This extra term is a correction to the spin-orbit force.

As shown in Refs.[16, 21], the basic result in the QMC model is that, in the scalar (σ) and vector (ω) meson fields, the nucleon behaves essentially as a point-like particle with an effective mass M_N^* , which depends on the position through only the σ field, moving in a vector potential generated by the ω meson, as mentioned near Eq.(4). Although we discussed the QMC model using the specific model, namely the bag model, in Ref.[16, 21], *the qualitative features we found are correct in any model* in which the nucleon contains *relativistic quarks* and the (middle- and long-range) *attractive* and (short-range) *repulsive* N-N forces have *Lorentz-scalar* and *vector characters*, respectively.

Let us suppose that the scalar and vector potentials in Eq.(3) are mediated by the σ and ω mesons, and introduce their mean-field values, which now depend on position \vec{r} , by $V_s^q(\vec{r}) = g_\sigma^q \sigma(\vec{r})$ and $V_v^q(\vec{r}) = g_\omega^q \omega(\vec{r})$, respectively, where g_σ^q (g_ω^q) is the coupling constant of the quark- σ (ω) meson. Furthermore, we shall add the isovector, vector meson, ρ , and the Coulomb field, $A(\vec{r})$, to describe finite nuclei realistically [16, 21]. Then, the effective Lagrangian density for finite nuclei, involving the quark degrees of freedom in the nucleon

and the (structureless) meson fields, in MFA would be given by [21]

$$\begin{aligned}
\mathcal{L}_{QMC-I} &= \bar{\psi}[i\gamma \cdot \partial - M_N^*(\sigma(\vec{r})) - g_\omega \omega(\vec{r})\gamma_0 \\
&\quad - g_\rho \frac{\tau_3^N}{2} b(\vec{r})\gamma_0 - \frac{e}{2}(1 + \tau_3^N)A(\vec{r})\gamma_0]\psi \\
&\quad - \frac{1}{2}[(\nabla\sigma(\vec{r}))^2 + m_\sigma^2\sigma(\vec{r})^2] + \frac{1}{2}[(\nabla\omega(\vec{r}))^2 + m_\omega^2\omega(\vec{r})^2] \\
&\quad + \frac{1}{2}[(\nabla b(\vec{r}))^2 + m_\rho^2 b(\vec{r})^2] + \frac{1}{2}(\nabla A(\vec{r}))^2,
\end{aligned} \tag{5}$$

where $\psi(\vec{r})$ and $b(\vec{r})$ are respectively the nucleon and the ρ (the time component in the third direction of isospin) fields. m_σ , m_ω and m_ρ are respectively the (constant) masses of the σ , ω and ρ mesons. g_ω and g_ρ are respectively the ω -N and ρ -N coupling constants, which are related to the corresponding quark- ω , g_ω^q , and quark- ρ , g_ρ^q , coupling constants as $g_\omega = 3g_\omega^q$ and $g_\rho = g_\rho^q$ [16, 21]. We call this model the QMC-I model. If we define the field-dependent σ -N coupling constant, $g_\sigma(\sigma)$, by

$$M_N^*(\sigma(\vec{r})) \equiv M_N - g_\sigma(\sigma(\vec{r}))\sigma(\vec{r}), \tag{6}$$

where M_N is the free nucleon mass, it is easy to compare with QHD [14]. $g_\sigma(\sigma)$ will be discussed further below.

The difference between QMC-I and QHD lies only in the coupling constant g_σ , which depends on the scalar field in QMC-I while it is constant in QHD. (The relationship between QMC and QHD has been already clarified in Ref.[19]. See also Ref.[23].) However, this difference leads to a lot of favorable results, notably the nuclear compressibility, [16, 18, 19, 21]. Detailed calculated properties of both infinite nuclear matter and finite nuclei can be found in Refs.[16, 21].

Here we consider the nucleon mass in matter further. The nucleon mass is a function of the scalar field. Because the scalar field is small at low density the nucleon mass can be expanded in terms of σ as

$$M_N^* = M_N + \left(\frac{\partial M_N^*}{\partial \sigma}\right)_{\sigma=0} \sigma + \frac{1}{2} \left(\frac{\partial^2 M_N^*}{\partial \sigma^2}\right)_{\sigma=0} \sigma^2 + \dots \tag{7}$$

In the QMC model the interaction Hamiltonian between the nucleon and the σ field at the quark level is given by $H_{int} = -3g_\sigma^q \int d\vec{r} \bar{\psi}_q \sigma \psi_q$, and the derivative of M_N^* with respect

to σ is

$$\left(\frac{\partial M_N^*}{\partial \sigma}\right) = -3g_\sigma^q \int d\vec{r} \bar{\psi}_q \psi_q \equiv -3g_\sigma^q S_N(\sigma). \quad (8)$$

Here we have defined the quark-scalar density in the nucleon, $S_N(\sigma)$, which is itself a function of the scalar field, by Eq.(8). Because of a negative value of $\left(\frac{\partial M_N^*}{\partial \sigma}\right)$, the nucleon mass decreases in matter at low density.

Furthermore, we define the scalar-density ratio, $S_N(\sigma)/S_N(0)$, to be $C_N(\sigma)$ and the σ -N coupling constant at $\sigma = 0$ to be g_σ (i.e., $g_\sigma \equiv g_\sigma(\sigma = 0)$):

$$C_N(\sigma) = S_N(\sigma)/S_N(0) \quad \text{and} \quad g_\sigma = 3g_\sigma^q S_N(0). \quad (9)$$

Comparing with Eq.(6), we find that

$$\left(\frac{\partial M_N^*}{\partial \sigma}\right) = -g_\sigma C_N(\sigma) = -\frac{\partial}{\partial \sigma} [g_\sigma(\sigma)\sigma], \quad (10)$$

and that the nucleon mass is

$$M_N^* = M_N - g_\sigma \sigma - \frac{1}{2} g_\sigma C'_N(0) \sigma^2 + \dots \quad (11)$$

In general, C_N is a decreasing function because the quark in matter is more relativistic than in free space. Thus, $C'_N(0)$ takes a negative value. If the nucleon were structureless C_N would not depend on the scalar field, that is, C_N would be constant ($C_N = 1$). Therefore, only the first two terms in the right hand side of Eq.(11) remain, which is exactly the same as the equation for the effective nucleon mass in QHD. By taking the heavy-quark-mass limit in QMC we can reproduce the QHD results [19].

If the MIT bag model is adopted as the nucleon model, S_N is explicitly given by [19, 24]

$$S_N(\sigma) = \frac{\Omega^*/2 + m_q^* R_N^* (\Omega^* - 1)}{\Omega^* (\Omega^* - 1) + m_q^* R_N^* / 2}, \quad (12)$$

where $\Omega^* = \sqrt{x_N^{*2} + (R_N^* m_q^*)^2}$ is the kinetic energy of the quark in units of $1/R_N^*$ and x_N^* is the eigenvalue of the quark in the nucleon in matter. We denote the bag radius of the nucleon in free space (matter) by R_N (R_N^*). In actual numerical calculations we found that the scalar-density ratio, $C_N(\sigma)$, decreases linearly (to a very good approximation)

with $g_\sigma\sigma$ [16, 21]. Then, it is very useful to have a simple parametrization for C_N :

$$C_N(\sigma) = 1 - a_N \times (g_\sigma\sigma), \quad (13)$$

with $g_\sigma\sigma$ in MeV (recall $g_\sigma = g_\sigma(\sigma = 0)$) and $a_N \sim 9 \times 10^{-4}$ (MeV $^{-1}$) for $m_q = 5$ MeV and $R_N = 0.8$ fm. This is quite accurate up to $\sim 3\rho_0$.

As a practical matter, it is easy to solve Eq.(10) for $g_\sigma(\sigma)$ in the case where $C(\sigma)$ is linear in $g_\sigma\sigma$, as in Eq.(13). Then one finds

$$M_N^* = M_N - g_\sigma \left[1 - \frac{a_N}{2}(g_\sigma\sigma) \right] \sigma, \quad (14)$$

so that the effective σ -N coupling constant, $g_\sigma(\sigma)$, decreases at half the rate of $C_N(\sigma)$.

II.2 Effect of meson structure

In the previous section we have considered the effect of nucleon structure. It is however true that the mesons are also built of quarks and anti-quarks, and that they may change their properties in matter.

To incorporate the effect of meson structure in the QMC model, we suppose that the vector mesons are again described by a relativistic quark model with *common* scalar and vector mean-fields [20], like the nucleon (see Eq.(3)). Then, again the effective vector-meson mass in matter, $m_v^*(v = \omega, \rho)$, depends on only the scalar mean-field.

However, for the scalar (σ) meson it may not be easy to describe it by a simple quark model (like a bag) because it couples strongly to the pseudoscalar (2π) channel, which requires a direct treatment of chiral symmetry in medium [25]. Since, according to the Nambu–Jona-Lasinio model [25, 26] or the Walecka model [8], one might expect the σ -meson mass in medium, m_σ^* , to be less than the free one, we shall here parametrize it using a quadratic function of the scalar field:

$$\left(\frac{m_\sigma^*}{m_\sigma} \right) = 1 - a_\sigma(g_\sigma\sigma) + b_\sigma(g_\sigma\sigma)^2, \quad (15)$$

with $g_\sigma\sigma$ in MeV, and we introduce two parameters, a_σ (in MeV $^{-1}$) and b_σ (in MeV $^{-2}$). (We will determine these parameters in the next section.)

Using these effective meson masses, we can find a new Lagrangian density for finite nuclei, which involves the structure effects of not only the nucleons but also the mesons, in the MFA:

$$\begin{aligned}
\mathcal{L}_{QMC-II} &= \bar{\psi}[i\gamma \cdot \partial - M_N^* - g_\omega \omega(\vec{r})\gamma_0 - g_\rho \frac{\tau_3^N}{2} b(\vec{r})\gamma_0 - \frac{e}{2}(1 + \tau_3^N)A(\vec{r})\gamma_0]\psi \\
&- \frac{1}{2}[(\nabla\sigma(\vec{r}))^2 + m_\sigma^{*2}\sigma(\vec{r})^2] + \frac{1}{2}[(\nabla\omega(\vec{r}))^2 + m_\omega^{*2}\omega(\vec{r})^2] \\
&+ \frac{1}{2}[(\nabla b(\vec{r}))^2 + m_\rho^{*2}b(\vec{r})^2] + \frac{1}{2}(\nabla A(\vec{r}))^2,
\end{aligned} \tag{16}$$

where the masses of the mesons and the nucleon depend on the scalar mean-fields. We call this model QMC-II.

At low density the vector-meson mass can be again expanded in the same way as in the nucleon case (Eq.(7)):

$$\begin{aligned}
m_v^* &= m_v + \left(\frac{\partial m_v^*}{\partial \sigma}\right)_{\sigma=0} \sigma + \frac{1}{2} \left(\frac{\partial^2 m_v^*}{\partial \sigma^2}\right)_{\sigma=0} \sigma^2 + \dots, \\
&\simeq m_v - 2g_\sigma^q S_v(0)\sigma - g_\sigma^q S_v'(0)\sigma^2, \\
&\equiv m_v - \frac{2}{3}g_\sigma \Gamma_{v/N}\sigma - \frac{1}{3}g_\sigma \Gamma_{v/N} C_v'(0)\sigma^2,
\end{aligned} \tag{17}$$

where $S_v(\sigma)$ is the quark-scalar density in the vector meson,

$$\left(\frac{\partial m_v^*}{\partial \sigma}\right) = -\frac{2}{3}g_\sigma \Gamma_{v/N} C_v(\sigma), \tag{18}$$

and $C_v(\sigma) = S_v(\sigma)/S_v(0)$. In Eqs.(17) and (18), we introduce a correction factor, $\Gamma_{v/N}$, which is given by $S_v(0)/S_N(0)$, because the coupling constant, g_σ , is defined specifically for the nucleon by Eq.(9).

III NUMERICAL RESULTS

In this section we will show our numerical results using the Lagrangian density of the QMC-II model that is, including self-consistently the density dependence of the meson masses. We have studied the QMC-I model, and have already shown the calculated properties of finite nuclei in Refs.[16, 21].

III.1 Infinite nuclear matter

For infinite nuclear matter we take the Fermi momenta for protons and neutrons to be k_{F_i} ($i = p$ or n). This is defined by $\rho_i = k_{F_i}^3/(3\pi^2)$, where ρ_i is the density of protons or neutrons, and the total baryon density, ρ_B , is then given by $\rho_p + \rho_n$. Let the *constant* mean-field values for the σ , ω and ρ fields be $\bar{\sigma}$, $\bar{\omega}$ and \bar{b} , respectively.

From the Lagrangian density Eq.(16), the total energy per nucleon, E_{tot}/A , can be written (without the Coulomb force)

$$E_{tot}/A = \frac{2}{\rho_B(2\pi)^3} \sum_{i=p,n} \int^{k_{F_i}} d\vec{k} \sqrt{M_i^{*2} + \vec{k}^2} + \frac{m_\sigma^{*2}}{2\rho_B} \bar{\sigma}^2 + \frac{g_\omega^2}{2m_\omega^{*2}} \rho_B + \frac{g_\rho^2}{8m_\rho^{*2}} \rho_3^2, \quad (19)$$

where the value of the ω field is now determined by baryon number conservation as $\bar{\omega} = g_\omega \rho_B / m_\omega^{*2}$, and the ρ -field value by the difference in proton and neutron densities, $\rho_3 = \rho_p - \rho_n$, as $\bar{b} = g_\rho \rho_3 / (2m_\rho^{*2})$ [20].

On the other hand, the scalar mean-field is given by a self-consistency condition (SCC):

$$\begin{aligned} \bar{\sigma} = & - \frac{2}{(2\pi)^3 m_\sigma^{*2}} \left[\sum_{i=p,n} \int^{k_{F_i}} d\vec{k} \frac{M_i^*}{\sqrt{M_i^{*2} + \vec{k}^2}} \left(\frac{\partial M_i^*}{\partial \bar{\sigma}} \right) \right] \\ & + \frac{g_\omega^2 \rho_B^2}{m_\omega^{*3} m_\sigma^{*2}} \left(\frac{\partial m_\omega^*}{\partial \bar{\sigma}} \right) + \frac{g_\rho^2 \rho_3^2}{4m_\rho^{*3} m_\sigma^{*2}} \left(\frac{\partial m_\rho^*}{\partial \bar{\sigma}} \right) - \frac{\bar{\sigma}^2}{m_\sigma^*} \left(\frac{\partial m_\sigma^*}{\partial \bar{\sigma}} \right). \end{aligned} \quad (20)$$

Using Eqs.(10), (15) and (18), Eq.(20) can be rewritten

$$\begin{aligned} \bar{\sigma} = & \frac{2g_\sigma}{(2\pi)^3 m_\sigma^{*2}} \left[\sum_{i=p,n} C_i(\bar{\sigma}) \int^{k_{F_i}} d\vec{k} \frac{M_i^*}{\sqrt{M_i^{*2} + \vec{k}^2}} \right] + g_\sigma \left(\frac{m_\sigma}{m_\sigma^*} \right) [a_\sigma - 2b_\sigma(g_\sigma \bar{\sigma})] \bar{\sigma}^2 \\ & - \frac{2}{3} \left(\frac{g_\sigma}{m_\sigma^{*2}} \right) \left[\frac{g_\omega^2 \rho_B^2}{m_\omega^{*3}} \Gamma_{\omega/N} C_\omega(\bar{\sigma}) + \frac{g_\rho^2 \rho_3^2}{4m_\rho^{*3}} \Gamma_{\rho/N} C_\rho(\bar{\sigma}) \right]. \end{aligned} \quad (21)$$

Now we need a model for the structure of the hadrons involved. We use the MIT bag model in static, spherical cavity approximation [27]. As in Ref.[21], the bag constant B and the parameter z_N (which accounts for the sum of the c.m. and gluon fluctuation corrections [16]) in the familiar form of the MIT bag model Lagrangian are fixed to reproduce the free nucleon mass ($M_N = 939$ MeV) under the condition that the hadron mass be stationary under variation of the free bag radius (R_N in the case of the nucleon). Furthermore, to fit the free vector-meson masses, $m_\omega = 783$ MeV and $m_\rho = 770$ MeV, we

introduce new z -parameters for them, z_ω and z_ρ . In the following we choose $R_N = 0.8$ fm and the free quark mass $m_q = 5$ MeV. Variations of the quark mass and R_N only lead to numerically small changes in the calculated results [21]. We then find that $B^{1/4} = 170.0$ MeV, $z_N = 3.295$, $z_\omega = 1.907$ and $z_\rho = 1.857$. Thus, C_N is given by Eq.(12), and C_v is given by a similar form, with the kinetic energy of quark and the bag radius for the vector meson. We find that the bag model gives $\Gamma_{\omega,\rho/N} = 0.9996$. Therefore, we may discard those correction factors in practical calculations.

Next we must choose the two parameters in the parametrization for the σ -meson mass in matter (see Eq.(15)). In this paper, we consider three parameter sets: (A) $a_\sigma = 3.0 \times 10^{-4}$ (MeV $^{-1}$) and $b_\sigma = 100 \times 10^{-8}$ (MeV $^{-2}$), (B) $a_\sigma = 5.0 \times 10^{-4}$ (MeV $^{-1}$) and $b_\sigma = 50 \times 10^{-8}$ (MeV $^{-2}$), (C) $a_\sigma = 7.5 \times 10^{-4}$ (MeV $^{-1}$) and $b_\sigma = 100 \times 10^{-8}$ (MeV $^{-2}$). The parameter sets A, B and C give about 2%, 7% and 10% decreases of the σ mass at saturation density, respectively. We will revisit this issue in the next subsection.

Now we are in a position to determine the coupling constants. g_σ^2 and g_ω^2 are fixed to fit the binding energy (-15.7 MeV) at the saturation density ($\rho_0 = 0.15$ fm $^{-3}$) for symmetric nuclear matter. Furthermore, the ρ -meson coupling constant is used to reproduce the bulk symmetry energy, 35 MeV. We take $m_\sigma = 550$ MeV. The coupling constants and some calculated properties for matter are listed in Table 1. The last three columns show the relative changes (from their values at zero density) of the nucleon-bag radius ($\delta R_N^*/R_N$), the lowest eigenvalue ($\delta x_N^*/x_N$) and the root-mean-square radius (rms radius) of the nucleon calculated using the quark wave function ($\delta r_q^*/r_q$) at saturation density. We note that the nuclear compressibility is higher than that in QMC-I ($K \sim 200 - 300$ MeV) [21]. However, it is still much lower than in QHD [14]. As in QMC-I, the bag radius of the nucleon shrinks a little, while its rms radius swells a little. On the other hand, because of the scalar field, the eigenvalue is reduced more than 10% (at ρ_0) from that in free space.

The strength of the scalar mean-field, $g_\sigma \bar{\sigma}$, in medium is shown in Fig.1. At small density it is well approximated by a linear function of the density:

$$g_\sigma \bar{\sigma} \approx 200 \text{ (MeV)} \left(\frac{\rho_B}{\rho_0} \right). \quad (22)$$

Table 1: Coupling constants and calculated properties for symmetric nuclear matter at normal nuclear density ($m_q = 5$ MeV, $R_N = 0.8$ fm and $m_\sigma = 550$ MeV). The effective nucleon mass, M_N^* , and the nuclear compressibility, K , are quoted in MeV. The bottom row is for QHD.

type	$g_\sigma^2/4\pi$	$g_\omega^2/4\pi$	$g_\rho^2/4\pi$	M_N^*	K	$\delta R_N^*/R_N$	$\delta x_N^*/x_N$	$\delta r_q^*/r_q$
A	3.84	2.70	5.54	801	325	-0.01	-0.11	0.02
B	3.94	3.17	5.27	781	382	-0.01	-0.13	0.02
C	3.84	3.31	5.18	775	433	-0.02	-0.14	0.02
QHD	7.29	10.8	2.93	522	540	—	—	—

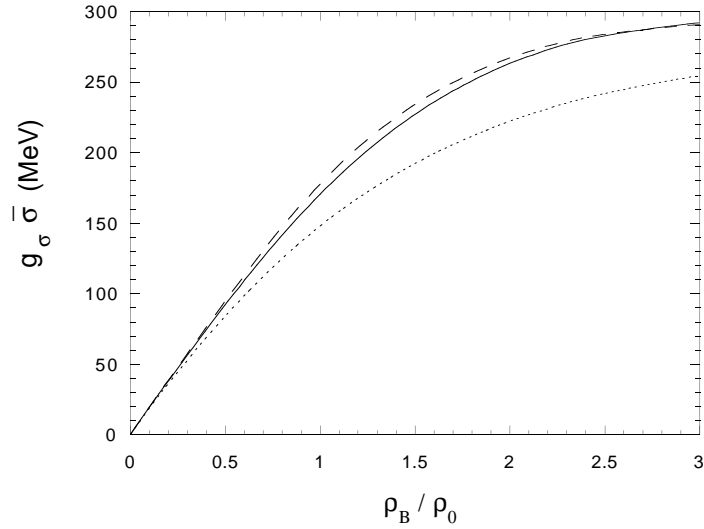


Figure 1: Scalar mean-field values. The dotted, solid and dashed curves are, respectively, for type A, B and C – as discussed below Eq.(21).

III.2 A new scaling phenomenon for hadron masses in matter

First, we show the dependence of the σ -meson mass on the nuclear density in Fig.2. Using

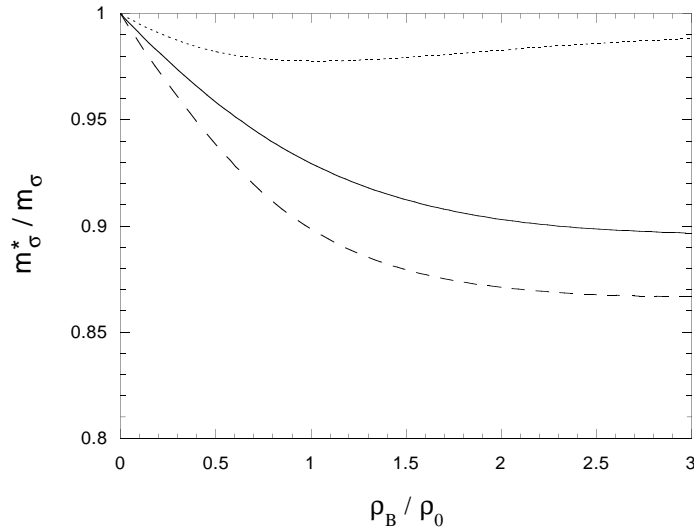


Figure 2: Effective σ -meson mass in symmetric nuclear matter. The curves are labelled as in Fig.1.

Eqs.(15) and (22), we find the σ mass at low density is

$$\left(\frac{m_\sigma^*}{m_\sigma}\right) \simeq 1 - \alpha_\sigma \left(\frac{\rho_B}{\rho_0}\right), \quad (23)$$

where $\alpha_\sigma = (0.06, 0.1, 0.15)$ for parameter set (A, B, C), respectively.

The effective nucleon mass is shown in Fig.3. It decreases as the density goes up, and behaves like a constant at large density. At small density it is approximately given by using Eqs.(14) and (22):

$$\left(\frac{M_N^*}{M_N}\right) \simeq 1 - 0.21 \left(\frac{\rho_B}{\rho_0}\right). \quad (24)$$

In Fig.4 the effective ω -meson mass is shown as a function of the density. (Since the difference between the effective ω - and ρ -meson masses at the same density is very small, we show only one curve for both mesons in the figure.) As the density increases the vector-meson mass decreases (as several authors have previously noticed [6, 7, 8, 9, 10, 11, 12])

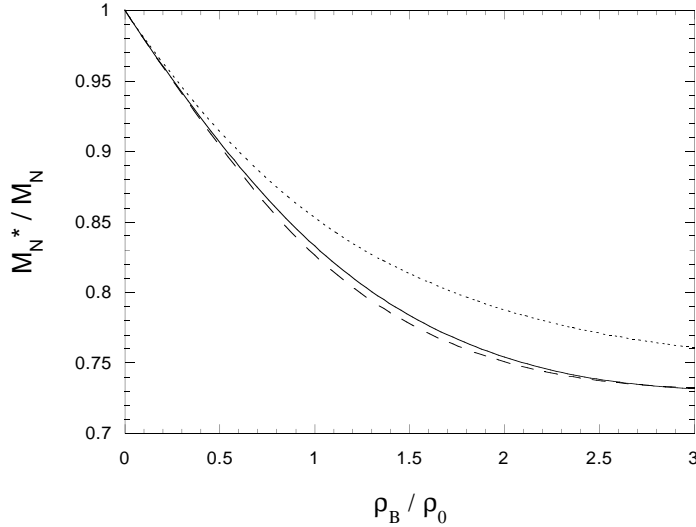


Figure 3: Effective nucleon mass in symmetric nuclear matter. The curves are labelled as in Fig.1.

and seems to become flat like the effective nucleon mass. Again, using Eqs.(17) and (22), the mass reduction can be well approximated by a linear form at small density:

$$\left(\frac{m_v^*}{m_v}\right) \simeq 1 - 0.17 \left(\frac{\rho_B}{\rho_0}\right). \quad (25)$$

The reduction factor, 0.17, is consistent with other models which have been applied to the same problem [12].

In Fig.5 we show the ratios of the quark-scalar density in medium to that in free space for the nucleon (C_N) and the ω meson (C_ω). As pointed out previously, we can easily see that the ratio for the nucleon is well approximated by a linear function of $g_\sigma\sigma$. It is also true that the ratio for the vector meson can be well described by a similar, linear function of $g_\sigma\sigma$:

$$C_v(\sigma) = 1 - a_v \times (g_\sigma\sigma). \quad (26)$$

We will see this parametrization again later.

In the present model it is possible to calculate masses of other hadrons. In particular, there is considerable interest in studying the masses of hyperons in medium – eg. Λ , Σ

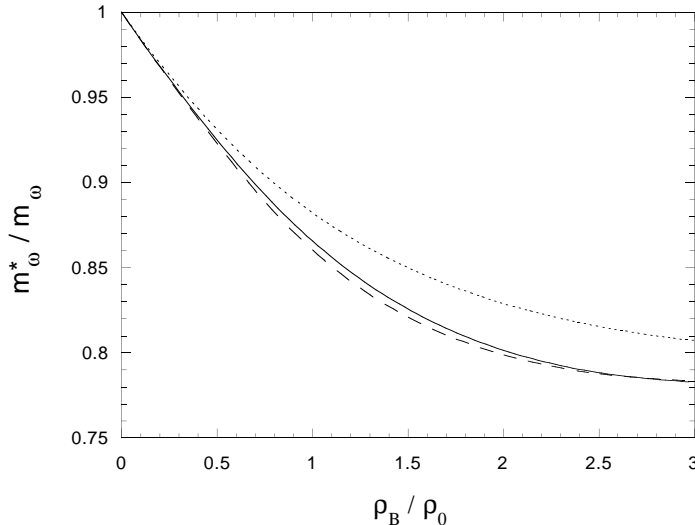


Figure 4: Effective (ρ - or) ω -meson mass in symmetric nuclear matter. The curves are labelled as in Fig.1.

and Ξ . For the hyperons themselves we again use the MIT bag model. We assume that the strange quark in the hyperon does not directly couple to the scalar field in MFA, as one would expect if the σ -meson represented a two-pion-exchange potential. It is also assumed that the addition of a single hyperon to nuclear matter of density ρ_B does not alter the values of the scalar and vector mean-fields, namely, we take the local-density approximation to the hyperons [28]. The mass of the strange quark, m_s , is taken to be $m_s = 250$ MeV, and new z -parameters in the mass formula are again introduced to reproduce the free hyperon masses: $z_\Lambda = 3.131$, $z_\Sigma = 2.810$, and $z_\Xi = 2.860$. Using those parameters, we have calculated the masses of Λ , Σ and Ξ in symmetric nuclear matter. They are presented in Fig.6. As for the nucleon and the vector mesons, the effective mass of the hyperon is determined by only the scalar field.

In general, we thus find that the effective hadron mass in medium is given by

$$\begin{aligned}
 M_j^* &= M_j + \left(\frac{\partial M_j^*}{\partial \sigma} \right)_{\sigma=0} \sigma + \frac{1}{2} \left(\frac{\partial^2 M_j^*}{\partial \sigma^2} \right)_{\sigma=0} \sigma^2 + \dots, \\
 &\simeq M_j - \frac{n_0}{3} g_\sigma \Gamma_{j/N} \sigma - \frac{n_0}{6} g_\sigma \Gamma_{j/N} C'_j(0) \sigma^2,
 \end{aligned} \tag{27}$$

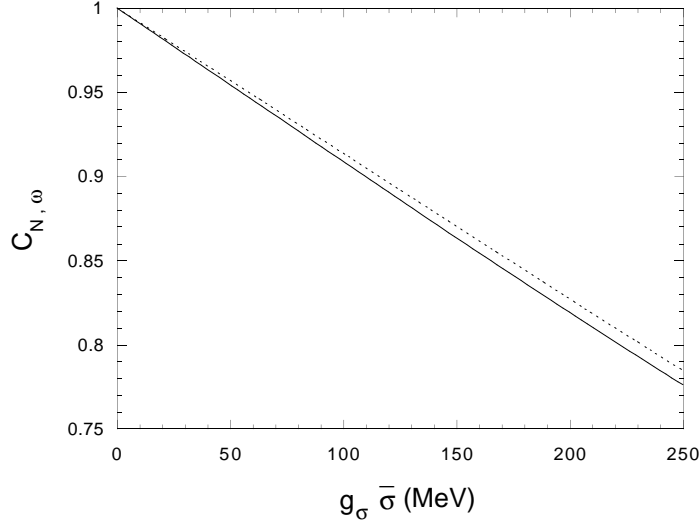


Figure 5: The ratios of the quark-scalar density in medium to that in free space for the nucleon (solid curve) and the ω meson (dotted curve) – using parameter set B.

where j stands for N , ω , ρ , Λ , Σ , Ξ , etc., n_0 is the number of non-strange quarks in the hadron j , $\Gamma_{j/N} = S_j(0)/S_N(0)$ with the quark-scalar density, S_j , in j , and the scalar density ratio, $C_j(\sigma) = S_j(\sigma)/S_j(0)$.

Using Eqs.(22) and (27), we find that the hyperon masses at low density are given by

$$\left(\frac{M_\Lambda^*}{M_\Lambda}\right) \simeq 1 - 0.12 \left(\frac{\rho_B}{\rho_0}\right), \quad (28)$$

$$\left(\frac{M_\Sigma^*}{M_\Sigma}\right) \simeq 1 - 0.11 \left(\frac{\rho_B}{\rho_0}\right), \quad (29)$$

and

$$\left(\frac{M_\Xi^*}{M_\Xi}\right) \simeq 1 - 0.05 \left(\frac{\rho_B}{\rho_0}\right), \quad (30)$$

where we take $\Gamma_{\Lambda, \Sigma, \Xi/N} = 1$, because we find that the Γ factor for the hyperon is again quite close to unity (e.g. $\Gamma_{\Lambda/N} = 1.0001$, in our actual calculations).

As seen in Fig.5 the linear approximation to the scalar-density ratio, C_j , is very convenient. We find that it is numerically relevant to not only the nucleon and the vector mesons but also the hyperons:

$$C_j(\sigma) = 1 - a_j \times (g_\sigma \sigma), \quad (31)$$

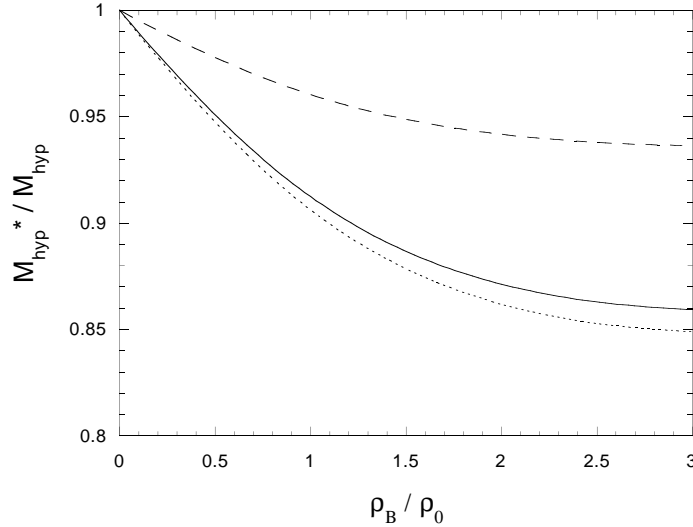


Figure 6: The ratio of the hyperon mass in medium to that in free space. The dotted, solid and dashed curves are respectively for the Λ , Σ , and Ξ hyperons, using parameter set B.

where a_j is the slope parameter for the hadron j . We list them in Table 2. We should

Table 2: Slope parameters for the hadrons ($\times 10^{-4}$ MeV $^{-1}$).

type	a_N	a_ω	a_ρ	a_Λ	a_Σ	a_Ξ
A	9.01	8.63	8.59	9.27	9.52	9.41
B	8.98	8.63	8.58	9.29	9.53	9.43
C	8.97	8.63	8.58	9.29	9.53	9.43

note that the dependence of a_j on the hadrons is quite weak, and it ranges around $8.6 \sim 9.5 \times 10^{-4}$ (MeV $^{-1}$).

If we ignore the weak dependence of a_j on the hadrons and take $\Gamma_{j/N} = 1$ in Eq.(27), the effective hadron mass can be rewritten in a quite simple form:

$$M_j^* \simeq M_j - \frac{n_0}{3}(g_\sigma\sigma) \left[1 - \frac{a}{2}(g_\sigma\sigma) \right], \quad (32)$$

where $a \simeq 9.0 \times 10^{-4}$ (MeV $^{-1}$). This mass formula can reproduce the hadron masses in matter quite well over a wide range of ρ_B , up to $\sim 3\rho_0$.

Since the scalar field is common to all hadrons, Eq.(32) leads to a new, simple scaling relationship among the hadron masses:

$$\left(\frac{\delta m_v^*}{\delta M_N^*}\right) \simeq \left(\frac{\delta M_\Lambda^*}{\delta M_N^*}\right) \simeq \left(\frac{\delta M_\Sigma^*}{\delta M_N^*}\right) \simeq \frac{2}{3} \quad \text{and} \quad \left(\frac{\delta M_\Xi^*}{\delta M_N^*}\right) \simeq \frac{1}{3}, \quad (33)$$

where $\delta M_j^* \equiv M_j - M_j^*$. The factors, $\frac{2}{3}$ and $\frac{1}{3}$, in Eq.(33) come from the ratio of the number of non-strange quarks in j to that in the nucleon. This means that the hadron mass is practically determined by only the number of non-strange quarks, which feel the common scalar field generated by surrounding nucleons in medium, and the strength of the scalar field [20]. On the other hand, the change in the confinement mechanism due to the environment gives a small contribution to the above ratio. It would be very interesting to see whether this scaling relationship is correct in forthcoming experiments.

III.3 Finite nuclei

In this subsection we will show our results for some finite, closed shell nuclei. The Lagrangian density, Eq.(16), leads to the following equations for finite nuclei:

$$\begin{aligned} \frac{d^2}{dr^2}\sigma(r) + \frac{2}{r}\frac{d}{dr}\sigma(r) - m_\sigma^{*2}\sigma(r) &= -g_\sigma C_N \rho_s(r) - m_\sigma m_\sigma^* g_\sigma [a_\sigma - 2b_\sigma g_\sigma \sigma(r)]\sigma(r)^2 \\ &+ \frac{2}{3}g_\sigma [m_\omega^* \Gamma_{\omega/N} C_\omega \omega(r)^2 + m_\rho^* \Gamma_{\rho/N} C_\rho b(r)^2], \end{aligned} \quad (34)$$

$$\frac{d^2}{dr^2}\omega(r) + \frac{2}{r}\frac{d}{dr}\omega(r) - m_\omega^{*2}\omega(r) = -g_\omega \rho_B(r), \quad (35)$$

$$\frac{d^2}{dr^2}b(r) + \frac{2}{r}\frac{d}{dr}b(r) - m_\rho^{*2}b(r) = -\frac{g_\rho}{2}\rho_3(r), \quad (36)$$

$$\frac{d^2}{dr^2}A(r) + \frac{2}{r}\frac{d}{dr}A(r) = -e\rho_p(r), \quad (37)$$

where

$$\rho_s(r) = \sum_{\alpha}^{occ} d_\alpha(r) (|G_\alpha(r)|^2 - |F_\alpha(r)|^2), \quad (38)$$

$$\rho_B(r) = \sum_{\alpha}^{occ} d_\alpha(r) (|G_\alpha(r)|^2 + |F_\alpha(r)|^2), \quad (39)$$

$$\rho_3(r) = \sum_{\alpha}^{occ} d_\alpha(r) (-)^{t_\alpha - 1/2} (|G_\alpha(r)|^2 + |F_\alpha(r)|^2), \quad (40)$$

$$\rho_p(r) = \sum_{\alpha}^{occ} d_\alpha(r) (t_\alpha + \frac{1}{2}) (|G_\alpha(r)|^2 + |F_\alpha(r)|^2), \quad (41)$$

with $d_\alpha(r) = (2j_\alpha + 1)/4\pi r^2$, and

$$\begin{aligned} \frac{d}{dr}G_\alpha(r) + \frac{\kappa}{r}G_\alpha(r) - [\epsilon_\alpha - g_\omega \omega(r) - t_\alpha g_\rho b(r) - (t_\alpha + \frac{1}{2})eA(r) + M_N \\ - g_\sigma(\sigma(r))\sigma(r)]F_\alpha(r) = 0, \end{aligned} \quad (42)$$

$$\begin{aligned} \frac{d}{dr}F_\alpha(r) - \frac{\kappa}{r}F_\alpha(r) + [\epsilon_\alpha - g_\omega \omega(r) - t_\alpha g_\rho b(r) - (t_\alpha + \frac{1}{2})eA(r) - M_N \\ + g_\sigma(\sigma(r))\sigma(r)]G_\alpha(r) = 0. \end{aligned} \quad (43)$$

Here $G_\alpha(r)/r$ and $F_\alpha(r)/r$ are respectively the radial part of the upper and lower components of the solution to the Dirac equation for the nucleon:

$$\psi(\vec{r}) = \begin{pmatrix} i[G_\alpha(r)/r]\Phi_{\kappa m} \\ -[F_\alpha(r)/r]\Phi_{-\kappa m} \end{pmatrix} \xi_{t_\alpha}, \quad (44)$$

where ξ_{t_α} is a two-component isospinor and $\Phi_{\kappa m}$ is a spin spherical harmonic [29] (α labelling the quantum numbers and ϵ_α being the energy). Then, the normalization condition is

$$\int dr (|G_\alpha(r)|^2 + |F_\alpha(r)|^2) = 1. \quad (45)$$

As usual, κ specifies the angular quantum numbers and t_α the eigenvalue of the isospin operator $\tau_3^N/2$. Practically, m_σ^* , m_v^* and C_j are respectively given by Eqs.(15), (27) and (31), and $g_\sigma(\sigma(r))$ is

$$g_\sigma(\sigma(r)) = g_\sigma \left[1 - \frac{a_N}{2} (g_\sigma \sigma(r)) \right]. \quad (46)$$

The total energy of the system is then given by

$$\begin{aligned} E_{tot} &= \sum_{\alpha}^{occ} (2j_\alpha + 1) \epsilon_\alpha - \frac{1}{2} \int d\vec{r} [-g_\sigma D(\sigma(r)) \sigma(r) \\ &+ g_\omega \omega(r) \rho_B(r) + \frac{1}{2} g_\rho b(r) \rho_3(r) + eA(r) \rho_p(r)], \end{aligned} \quad (47)$$

where

$$\begin{aligned} D(\sigma(r)) &= C_N \rho_s(r) + m_\sigma m_\sigma^* [a_\sigma - 2b_\sigma g_\sigma \sigma(r)] \sigma(r)^2 \\ &- \frac{2}{3} [m_\omega^* \Gamma_{\omega/N} C_\omega \omega(r)^2 + m_\rho^* \Gamma_{\rho/N} C_\rho b(r)^2]. \end{aligned} \quad (48)$$

There are seven parameters to be determined: g_σ , g_ω , g_ρ , e , m_σ , m_ω and m_ρ . As in the case of infinite matter we take the experimental values: $m_\omega = 783$ MeV, $m_\rho = 770$ MeV and $e^2/4\pi = 1/137.036$. The coupling constants g_σ , g_ω and g_ρ are fixed to describe the nuclear matter properties and the bulk symmetry energy per baryon of 35 MeV (see Table 1).

The σ -meson mass however determines the range of the attractive interaction and changes in m_σ affect the nuclear-surface slope and its thickness. Therefore, as in the paper of Horowitz and Serot [29], we adjust m_σ to fit the measured rms charge radius of ^{40}Ca , $r_{ch}(^{40}\text{Ca}) = 3.48$ fm [30]. (Notice that variations of m_σ at fixed (g_σ/m_σ) have no effect on the infinite nuclear matter properties [21].) We summarize the parameters in Table 3.

Table 3: Model parameters for finite nuclei (for $m_q = 5$ MeV and $R_N = 0.8$ fm).

type	$g_\sigma^2/4\pi$	$g_\omega^2/4\pi$	$g_\rho^2/4\pi$	m_σ (MeV)
A	1.67	2.70	5.54	363
B	2.01	3.17	5.27	393
C	2.19	3.31	5.18	416

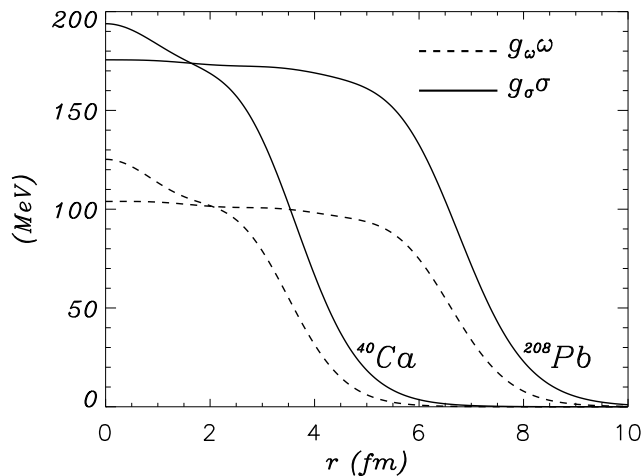


Figure 7: Scalar and vector strength for ^{40}Ca and ^{208}Pb (for type B).

Equations (35) to (45) give a set of coupled non-linear differential equations, which may be solved by a standard iteration procedure [31].

In Fig.7 we first show the calculated strength of the σ and ω fields in ^{40}Ca and ^{208}Pb . Next we show calculated charge density distributions, ρ_{ch} , of ^{40}Ca and ^{208}Pb in comparison with those of the experimental data in Figs.8 and 9. To see the difference among the results from the three parametrizations of m_σ^* (A, B and C), in Fig.8 we present only the interior part of $\rho_{ch}(^{40}\text{Ca})$. As in Ref.[21], we have used a convolution of the point-proton density, which is given by solving Eqs.(35) \sim (45), with the proton charge distribution to calculate ρ_{ch} . For ^{40}Ca the QMC-II model with parameter sets A and B give similar charge distributions to those in QMC-I, while the result of QMC-II with parameter set C

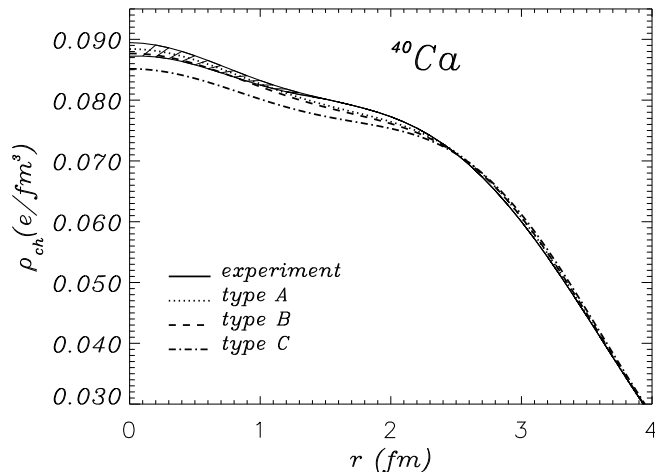


Figure 8: Charge density distribution for ^{40}Ca compared with the experimental data.

is closer to that in QHD. From Fig.9 we see that the present model also yields a charge distribution for ^{208}Pb which is similar to those calculated using QMC-I or QHD.

In Table 4, the calculated spectrum of ^{40}Ca is presented. Because of the relatively smaller scalar and vector fields in the present model than in QHD, the spin-orbit splittings are smaller (in this respect the model is very similar to QMC-I). We should note that there is a strong correlation between the effective nucleon mass and the spin-orbit force [21]. The problem concerning the spin-orbit force in the QMC model has been studied in Refs.[16, 21, 22, 23]. It remains to be seen whether the higher order corrections, as studied by Wallace et al. [32], will help to resolve it.

Table 5 gives a summary of the calculated binding energy per nucleon (E/A), rms charge radii and the difference between nuclear rms radii for neutrons and protons ($r_n - r_p$), for several closed-shell nuclei. While there are still some discrepancies between the results and data, the present model provides reasonable results. In particular, as in QMC-I, it reproduces the rms charge radii for medium and heavy nuclei quite well.

In Figs.10 and 11 we present the changes of the nucleon, σ and ω meson masses in ^{40}Ca and ^{208}Pb , respectively. The interior density of ^{40}Ca is much higher than ρ_0 , while that in ^{208}Pb is quite close to ρ_0 . Accordingly, in the interior the effective hadron masses

Table 4: Calculated proton and neutron spectra of ^{40}Ca (for type B) compared with QMC-I and the experimental data ($m_q = 5$ MeV and $R_N = 0.8$ fm). Here, I and II denote, respectively, QMC-I and QMC-II. All energies are in MeV.

Shell	neutron			proton		
	I	II	Expt.	I	II	Expt.
$1s_{1/2}$	43.1	41.1	51.9	35.2	33.2	50 ± 10
$1p_{3/2}$	31.4	30.0	36.6	23.8	22.3	34 ± 6
$1p_{1/2}$	30.2	29.0	34.5	22.5	21.4	34 ± 6
$1d_{5/2}$	19.1	18.0	21.6	11.7	10.6	15.5
$2s_{1/2}$	15.8	14.7	18.9	8.5	7.4	10.9
$1d_{3/2}$	17.0	16.4	18.4	9.7	9.0	8.3

Table 5: Binding energy per nucleon, $-E/A$ (in MeV), rms charge radius r_{ch} (in fm) and the difference between r_n and r_p (in fm) for type B, $m_q = 5$ MeV and $R_B = 0.8$ fm. I and II denote, respectively, QMC-I and QMC-II. (* fit)

model	$-E/A$			r_{ch}			$r_n - r_p$		
	I	II	Expt.	I	II	Expt.	I	II	Expt.
^{16}O	5.84	5.11	7.98	2.79	2.77	2.73	-0.03	-0.03	0.0
^{40}Ca	7.36	6.54	8.45	3.48*	3.48*	3.48	-0.05	-0.05	0.05 ± 0.05
^{48}Ca	7.26	6.27	8.57	3.52	3.53	3.47	0.23	0.24	0.2 ± 0.05
^{90}Zr	7.79	6.99	8.66	4.27	4.28	4.27	0.11	0.12	0.05 ± 0.1
^{208}Pb	7.25	6.52	7.86	5.49	5.49	5.50	0.26	0.27	0.16 ± 0.05

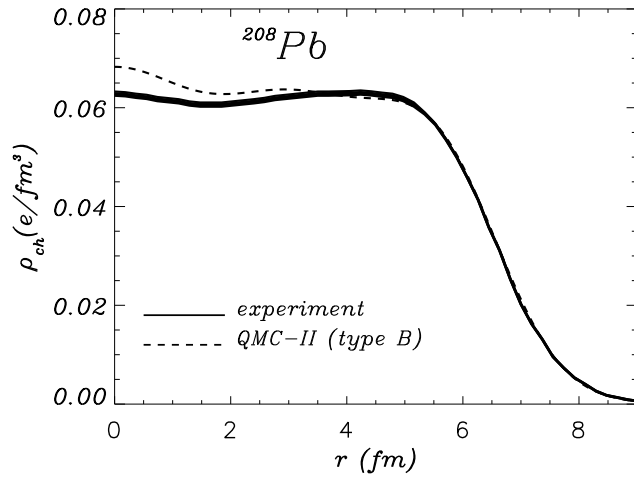


Figure 9: Same as Fig.8 but for ^{208}Pb . The parameter set B is used.

in ^{40}Ca are smaller than in ^{208}Pb . We can also see this in Fig.7, where the strength of the scalar field in the interior part of ^{40}Ca is stronger than in ^{208}Pb .

Using the local-density approximation and Eq.(32), it is possible to calculate the changes of the hyperon (Λ , Σ and Ξ) masses in ^{40}Ca and ^{208}Pb , which are respectively illustrated in Figs.12 and 13. Our quantitative calculations for the changes of the hyperon masses in finite nuclei may be quite important in forthcoming experiments concerning hypernuclei [28].

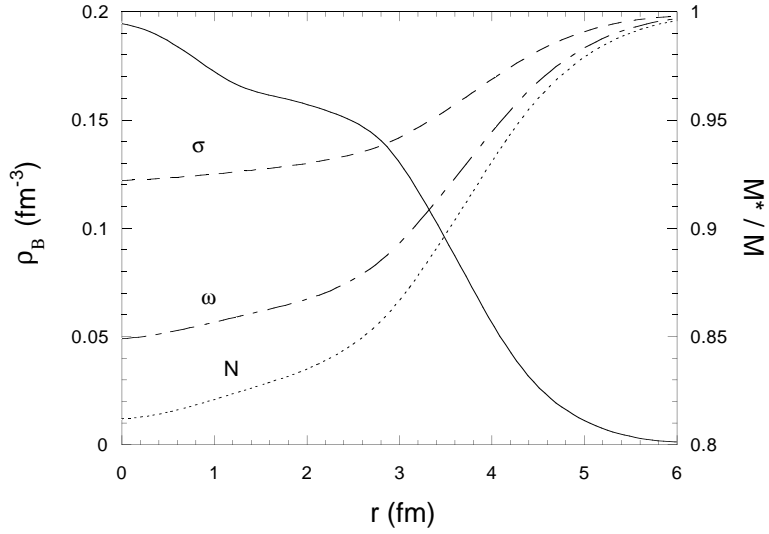


Figure 10: Changes of the nucleon, σ and ω meson masses in ^{40}Ca . The nuclear baryon density is also illustrated (solid curve). The right (left) scale is for the effective mass (the baryon density). The parameter set B is used.

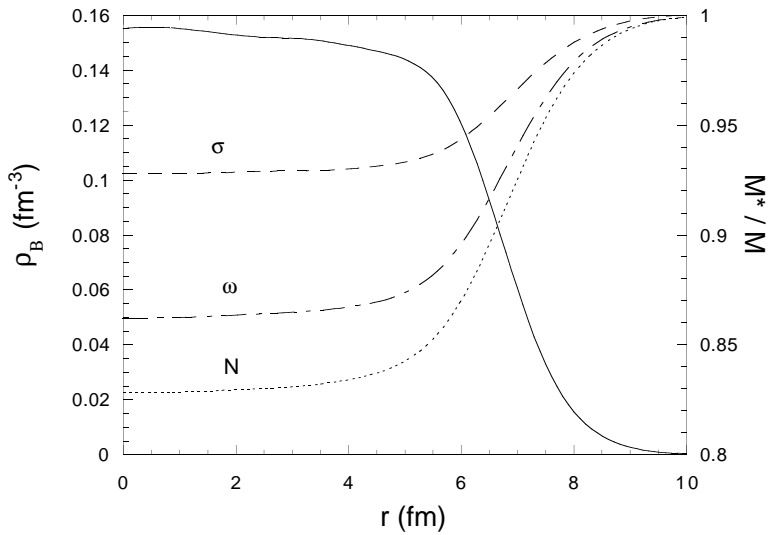


Figure 11: Same as Fig.10 but for ^{208}Pb .

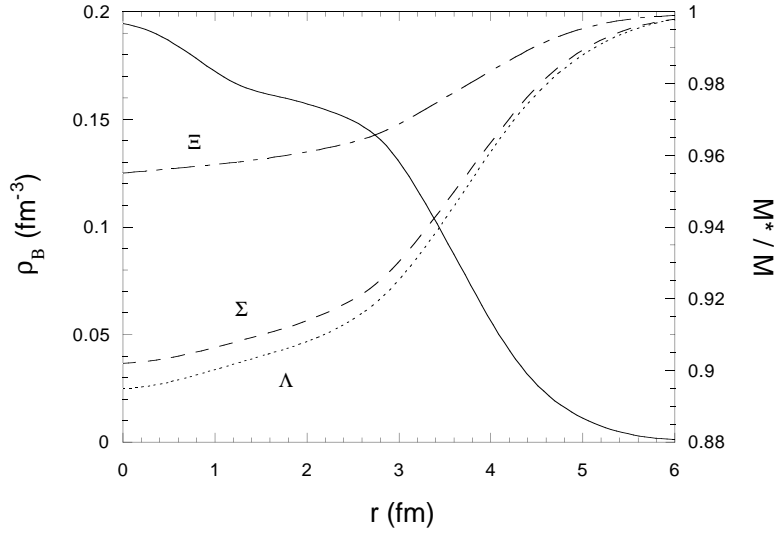


Figure 12: Changes of the hyperon (Λ , Σ and Ξ) masses in ^{40}Ca . The solid curve is for the nuclear baryon density. The right (left) scale is for the effective mass (the baryon density). The parameter set B is used.

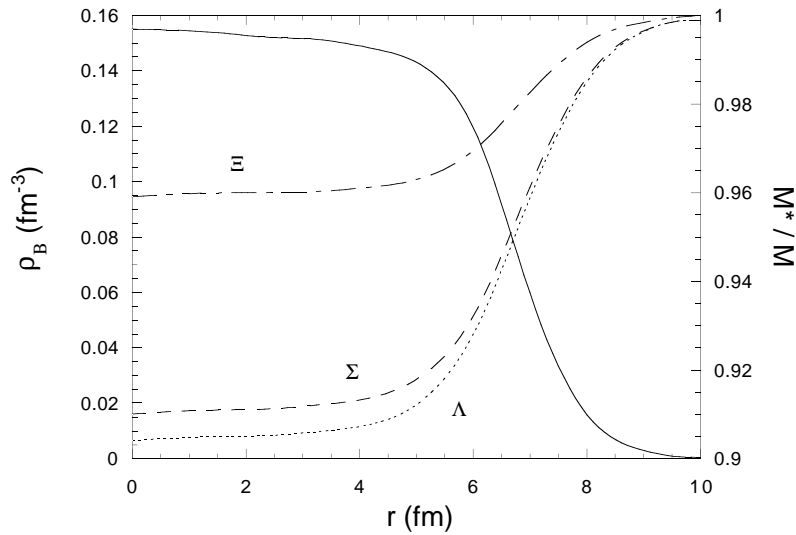


Figure 13: Same as Fig.12 but for ^{208}Pb .

IV CONCLUSION

We have extended the quark-meson coupling (QMC) model to include quark degrees of freedom within the scalar and vector mesons, as well as in the nucleons, and have investigated the density dependence of hadron masses in nuclear medium. As several authors have suggested [6, 7, 8, 9, 10, 11, 12, 20], the hadron mass is reduced because of the scalar mean-field in medium. Our results are quite consistent with the other models. In the present model the hadron mass can be related to the number of non-strange quarks and the strength of the scalar mean-field (see Eq.(32)). We have found a new, simple formula to describe the hadron masses in the medium, and this led to a new scaling relationship among them (see Eq.(33)). Furthermore, we have calculated the changes of not only the nucleon, σ , ω and ρ masses but also the hyperon (Λ , Σ and Ξ) masses in finite nuclei. We should note that the origins of the mass reduction in QMC and QHD are completely different [15]. It would be very interesting to compare our results with forthcoming experiments on hypernuclei.

By applying this extended QMC model to finite nuclei, we have studied the properties of some static, closed shell nuclei. Our (self-consistent) calculations reproduce well the observed static properties of nuclei such as the charge density distributions. In the present model, there are, however, still some discrepancies in energy spectra of nuclei, in particular, the spin-orbit splittings. To overcome this defect, we have discussed one possible way, in which a constituent quark mass (~ 300 MeV) is adopted, in Refs.[16, 21]. As an alternative, Jin and Jennings [23] and Blunden and Miller [22] have proposed variations of the bag constant and z parameter in medium, which have been suggested by the fact that quarks are partially deconfined in matter. To help settle this problem, one should perhaps consider the change of the vacuum properties in the medium [25].

Our Lagrangian density, Eq.(16), provides a lot of effective coupling terms among the meson fields because the mesons have structure (cf. Ref.[33]). In particular, the Lagrangian automatically offers self-coupling terms (or non-linear terms) with respect to the σ field. Using Eq.(15), the Lagrangian density gives the non-linear σ terms (up to

$\mathcal{O}(\sigma^4)$) as:

$$\begin{aligned}\mathcal{L}_{QMC-II}^{NL\sigma} &= -\frac{1}{2}m_\sigma^*(\sigma)^2\sigma^2, \\ &\simeq -\frac{1}{2}m_\sigma^2\sigma^2 + g_\sigma a_\sigma m_\sigma^2\sigma^3 - \frac{1}{2}g_\sigma^2(a_\sigma^2 + 2b_\sigma)m_\sigma^2\sigma^4.\end{aligned}\quad (49)$$

On the other hand, in nuclear physics, QHD with non-linear σ terms has been extensively used in MFA to describe realistic nuclei [34]. The most popular parametrizations are called NL1, NL2 [35] and NL-SH [36], and the non-linear terms in those parametrizations are given as

$$\mathcal{L}_{QHD}^{NL\sigma} = -\frac{1}{2}m_\sigma^2\sigma^2 + \frac{1}{3}g_2\sigma^3 + \frac{1}{4}g_3\sigma^4, \quad (50)$$

where g_2 and g_3 take respectively a positive (negative) [positive] and positive (negative) [positive] values in NL1 (NL2) [NL-SH]. Since the non-linear σ terms provide the self-energy of σ meson, it changes the σ mass in matter. Comparing Eq.(50) with Eq.(49), we can see that the effective σ mass in NL2 *increases* at low nuclear density while the σ mass *decreases* in NL1 and NL-SH in MFA.

However, from the point of view of a field theory, like the Nambu–Jona-Lasinio model, an increase of the σ mass in the medium seems unlikely [25, 26]. (We should note that the values of g_2 in those parametrizations are small compared with the corresponding one in Eq.(49).) Furthermore, from the point of view of field theory, g_3 in Eq.(50) should be negative because the vacuum must be stable [37]. Therefore, we can conclude that one would expect to find $g_2 \geq 0$ and $g_3 \leq 0$ in Eq.(50). Unfortunately, the above three parametrizations used in nuclear physics do not satisfy the condition, while our Lagrangian, Eq.(49), does. It will be very interesting to explore the connection between various coupling strengths found empirically in earlier work and those found in our approach.

Finally, we would like to give some caveats concerning the present calculation. The basic idea of the model is that the mesons are locally coupled to the quarks. Therefore, in the present model the effect of short-range correlations among the quarks, which would be associated with overlap of the hadrons, are completely neglected. At very high density these would be expected to dominate and the present model must eventually break down

there (probably beyond $\sim 3\rho_B/\rho_0$). Furthermore, the pionic cloud of the hadron [38] should be considered explicitly in any truly quantitative study of hadron properties in medium. We note that subtleties such as scalar-vector mixing in medium and the splitting between longitudinal and transverse masses of the vector mesons [10] have been ignored in the present mean-field study. Although the former appears to be quite small in QHD the latter will certainly be important in any attempt to actually measure the mass shift.

This work was supported by the Australian Research Council.

References

- [1] M. Masera (HELIOS-3 collaboration), Nucl. Phys. **A590**, 93c (1995).
- [2] P. Wurm (CERES collaboration), Nucl. Phys. **A590**, 103c (1995).
- [3] G.Q. Li, C.M. Ko and G.E. Brown, Nucl. Phys. **A606**, 568 (1996);
G. Chanfray, R. Rapp, and J. Wambach, Phys. Rev. Lett. **76**, 368 (1996).
- [4] Quark Matter '95, Nucl. Phys. **A590** (1995).
- [5] Lattice '94, Nucl. Phys. **B42** (Proc. Suppl.) (1995).
- [6] M. Asakawa, C.M. Ko, P. Lévai and X.J. Qiu, Phys. Rev. **C46**, R1159 (1992).
- [7] T. Hatsuda and Su H. Lee, Phys. Rev. **C46**, R34 (1993);
M. Asakawa and C.M. Ko, Phys. Rev. **C48**, R526 (1993);
T. Hatsuda, Y. Koike and Su H. Lee, Nucl. Phys. **B394**, 221 (1993).
- [8] K. Saito, T. Maruyama and K. Soutome, Phys. Rev. **C40**, 407 (1989);
K. Soutome, T. Maruyama and K. Saito, Nucl. Phys. **A507**, 731 (1990).
- [9] H. Kurasawa and T. Suzuki, Prog. Theor. Phys. **84**, 1030 (1990);
J.C. Caillon and J. Labarsouque, Phys. Lett. **B311**, 19 (1993).
- [10] H.-C. Jean, J. Piekarewicz and A.G. Williams, Phys. Rev. **C49**, 1981 (1994).
- [11] H. Shiomi and T. Hatsuda, Phys. Lett. **B334**, 281 (1994);
H. Kuwabara and T. Hatsuda, Prog. Theor. Phys. **96**, 1163 (1995).
- [12] T. Hatsuda, to be published in Proc. of the international symposium on Non-Nucleonic Degrees of Freedom Detected in Nucleus, Osaka, Sept. 2–5 (1996) (World Scientific, Singapore).
- [13] D.K. Griegel and Thomas. D. Cohen, Phys. Lett. **B333**, 27 (1994).

- [14] J.D. Walecka, Ann. Phys. (N.Y.) **83**, 491 (1974);
 B.D. Serot and J.D. Walecka, Advan. Nucl. Phys. **16**, 1 (1986).
- [15] K. Saito and A.W. Thomas, Phys. Rev. **C52**, 2789 (1995).
- [16] P.A.M. Guichon, K. Saito, E. Rodionov and A.W. Thomas, Nucl. Phys. **A601**, 349 (1996);
 P.A.M. Guichon, K. Saito and A.W. Thomas, nucl-th/9602022, to appear in Australian Journal of Physics (1996).
- [17] P.A.M. Guichon, Phys. Lett. **B200**, 235 (1988).
- [18] K. Saito, A. Michels and A.W. Thomas, Phys. Rev. **C46**, R2149 (1992);
 A.W. Thomas, K. Saito and A. Michels, Aust. J. Phys. **46**, 3 (1993);
 K. Saito and A.W. Thomas, Nucl. Phys. **A574**, 659 (1994); Phys. Lett. **B335**, 17 (1994); ibid. **B363**, 157 (1995).
- [19] K. Saito and A.W. Thomas, Phys. Lett. **B327**, 9 (1994).
- [20] K. Saito and A.W. Thomas, Phys. Rev. **C51**, 2757 (1995).
- [21] K. Saito, K. Tsushima and A.W. Thomas, Nucl. Phys. **A609**, 339 (1996).
- [22] P.G. Blunden and G.A. Miller, Phys. Rev. **C54**, 359 (1996).
- [23] X. Jin and B.K. Jennings, Phys. Lett. **B374** (1996) 13; Phys. Rev. **C54**, 1427 (1996);
 nucl-th/9608023.
- [24] In our earlier works, the phenomenological center-of-mass correction to the bag energy was used. In this paper, however, we do not use it because the c.m. and gluon fluctuation corrections may be absorbed into the familiar form, $-z_N/R_N$. See Ref.[16].
- [25] T. Hatsuda and T. Kunihiro, Phys. Rep. **247**, 221 (1994).
- [26] V. Bernard and Ulf-G. Meissner, Nucl. Phys. **A489**, 647 (1988).

- [27] A. Chodos, R.L. Jaffe, K. Johnson and C.B. Thorn, Phys. Rev. **D10**, 2599 (1974).
- [28] K. Tsushima, K. Saito and A.W. Thomas, A self-consistent calculation for hypernuclei, to be published.
- [29] C.J. Horowitz and B.D. Serot, Nucl. Phys. **A368**, 503 (1981);
C.J. Horowitz, D.P. Murdoch and B.D. Serot, Computational Nuclear Physics 1, eds. K. Langanke, J.A. Maruhn and S.E. Koonin (Springer-Verlag, Berlin, 1991), p.129.
- [30] B.B.P. Sinha *et al.*, Phys. Lett. **B53**, 217 (1971).
- [31] The numerical calculation was carried out by modifying the technique described by Horowitz *et al.* [29]. It was performed with a maximum radius of 12 (15) fm on a mesh of 0.04 fm for medium mass (Pb) nuclei. Since the numerical convergence is slow we have improved the program by mixing appropriately the meson potentials given by the i -th iteration and those by the $(i - 1)$ -th iteration – as is usually done in non-relativistic calculations. For the QMC-II model, it is needed to calculate several 10 iterations for middle nuclei while about 100 iterations for Pb. We find that it becomes harder to find a good initial condition for the meson fields in the case where the nuclear compressibility is smaller, for example, in the parameter set A rather than in C. Probably a more powerful technique is required to make the convergence of the calculation rapid.
- [32] D.R. Phillips, M.C. Birse and S.J. Wallace, nucl-th/9610007.
- [33] R.J. Furnstahl, B.D. Serot and H.-B. Tang, Nucl. Phys. **A598**, 539 (1996);
H. Müller and B.D. Serot, Nucl. Phys. **A606**, 508 (1996).
- [34] P.G. Reinhard, Rep. Prog. Phys. **52**, 439 (1989);
G.A. Lalazissis, M.M. Sharma, P. Ring and Y.K. Gambhir, Nucl. Phys. **A608**, 202 (1996).

- [35] S.J. Lee *et al.*, Phys. Rev. Lett. **57**, 2916 (1986);
P.G. Reinhard *et al.*, Z. Phys. **A323**, 13 (1986).
- [36] M.M. Sharma, M.A. Nagarajan and P. Ring, Phys. Lett. **B312**, 377 (1993).
- [37] T.D. Lee and G.C. Wick, Phys. Rev. **D9**, 2291 (1974).
- [38] A.W. Thomas, Advan. Nucl. Phys. **13**, 1 (1984);
G.A. Miller, Int. Rev. Nucl. Phys. **2**, 190 (1984).